

FlexHaptics: A Design Method for Passive Haptic Inputs Using Planar Compliant Structures

Hongnan Lin
Georgia Institute of Technology
Atlanta, USA
hlin324@gatech.edu

Yifan Li
Georgia Institute of Technology
Atlanta, USA
lyfan0924@gatech.edu

Wei Wang
Hunan University
Changsha, China
wei.wang@mmlab.cn

Liang He
University of Washington
Seattle, USA
lianghe@cs.washington.edu

Tingyu Cheng
Georgia Institute of Technology
Atlanta, USA
tcheng32@gatech.edu

Hyunjoo Oh
Georgia Institute of Technology
Atlanta, USA
hyunjoo.oh@gatech.edu

Fangli Song
Georgia Institute of Technology
Atlanta, USA
fsong35@gatech.edu

Clement Zheng
National University of Singapore
Singapore
clement.zheng@gmail.com



Figure 1: Example applications made with FlexHaptics method: (A) a piano keyboard interface for touchscreen musical applications, (B) a VR controller attachment for bow shooting games, and (C) a joystick with a two-step button on the stick end.

ABSTRACT

This paper presents FlexHaptics, a design method for creating custom haptic input interfaces. Our approach leverages planar compliant structures whose force-deformation relationship can be altered by adjusting the geometries. Embedded with such structures, a FlexHaptics module exerts a fine-tunable haptic effect (i.e., resistance, detent, or bounce) along a movement path (i.e., linear, rotary, or ortho-planar). These modules can work separately or combine into an interface with complex movement paths and haptic effects. To enable the parametric design of FlexHaptic modules, we provide a design editor that converts user-specified haptic properties into underlying mechanical structures of haptic modules. We validate our approach and demonstrate the potential of FlexHaptic modules through six application examples, including a slider control for a painting application and a piano keyboard interface on

touchscreens, a tactile low vision timer, VR game controllers, and a compound input device of a joystick and a two-step button.

CCS CONCEPTS

• **Human-centered computing** → **Systems and tools for interaction design.**

KEYWORDS

Haptics; Compliant structure; Parametric design; Digital fabrication; Tangible interface.

ACM Reference Format:

Hongnan Lin, Liang He, Fangli Song, Yifan Li, Tingyu Cheng, Clement Zheng, Wei Wang, and Hyunjoo Oh. 2022. FlexHaptics: A Design Method for Passive Haptic Inputs Using Planar Compliant Structures. In *CHI Conference on Human Factors in Computing Systems (CHI '22)*, April 29-May 5, 2022, New Orleans, LA, USA. ACM, New York, NY, USA, 13 pages. <https://doi.org/10.1145/3491102.3502113>

1 INTRODUCTION

Haptic feedback in tangible input interfaces is critical to enhancing user performance and engagement. With haptic feedback providing touch sensation, users make precise manipulation at ease [22], confirm a successful input without paying extra attention [5], and perceive extended responsiveness from an interactive system [23, 33]. However, off-the-shelf components with predetermined and fixed

Permission to make digital or hard copies of all or part of this work for personal or classroom use is granted without fee provided that copies are not made or distributed for profit or commercial advantage and that copies bear this notice and the full citation on the first page. Copyrights for components of this work owned by others than ACM must be honored. Abstracting with credit is permitted. To copy otherwise, or republish, to post on servers or to redistribute to lists, requires prior specific permission and/or a fee. Request permissions from permissions@acm.org.

CHI '22, April 29-May 5, 2022, New Orleans, LA, USA

© 2022 Association for Computing Machinery.

ACM ISBN 978-1-4503-9157-3/22/04...\$15.00

<https://doi.org/10.1145/3491102.3502113>

haptic profiles are insufficient to satisfy an increasing need for sophisticated interaction design for various user scenarios. Customizing passive haptic inputs, which have fixed force-movement profiles determined by mechanical mechanisms, expands design opportunities and also challenges to support a wider variety of haptic interfaces.

Some methods to create passive haptic inputs are to embed magnetic [20, 40, 41] and flexible [25, 31, 34] materials. Others using a single and regular material employ coil spring [12], kirigami [8], and metamaterial [14, 22, 32] mechanisms. The later ones facilitate prototyping as they enable designers to generate mechanisms with desired haptic properties with computer aid and fabricate their designs with widely accessible machines (i.e., 3D printers and laser cutters) and materials (i.e., PLA filaments and plastic sheets). To forward the computer-aided design and fabrication of haptic inputs with predictable force-feedback, we introduce a new method that leverages beam structures, superior in their simple geometries and predictable haptic properties.

We propose FlexHaptics method that supports creating haptic inputs with a set of mechanical module designs that provide predictable force-feedback with embedded beam structures (Figure 2). We present eight different modules. Each unit generates a different kind of haptic effects, including resistance, detent, or bounce, while traveling along a linear, rotary, ortho-planar linear movement path. The modules are planar and compact, therefore are easy to fabricate by 3D printing PLA, laser-cutting an acetal plastic (POM) sheet, or laser-cutting an acrylic sheet. The form factor also aligns with the construction of modern products, such as touchscreen devices, gamepads, and keyboards, and satisfies the common need of arranging multiple inputs within a small space. Moreover, we propose two mixing operators to guide designers on composing with the modules: parallel mixing generates an input with multiple haptic effects along a primitive path, and series mixing generates an input with a compound path.

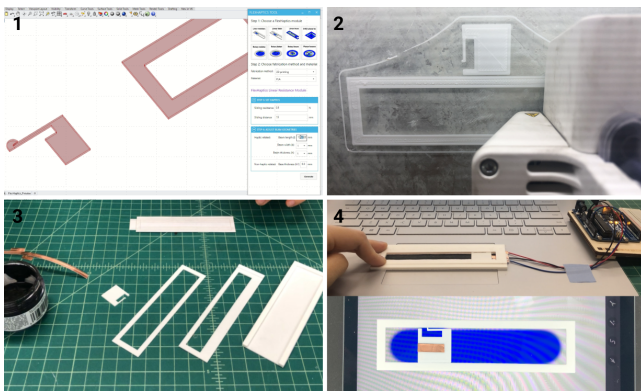


Figure 2: Flexhaptics workflow: 1) designing a module with desired haptic effects in FlexHaptics editor, 2) fabricating the module by 3D printing or laser cutting, 3) assembling the parts and embedding a circuit, 4) application example as a haptic slider used with a microcontroller (top) and on a touchscreen (bottom).

The method comprises an editor as a plug-in within Rhinoceros and Grasshopper to let designers explore module design according to desired force feedback. To implement the editor, first, we developed mathematical models quantifying the haptics-geometries relationship of each module. The models are in the format of linear regression analysis equations with an explanatory variable of a composite geometric component, informed by existing theories and models. Then we computed the coefficients and validated the models through finite element analysis (FEA) and experiments with modules fabricated with the three methods. Based on the experiment results, we adjusted the generation algorithms to address fabrication issues. Finally, we developed the back-end of the editor with Grasshopper and Rhinocommon in C# and the front-end interface with Human UI. The key contributions of this paper are as follows:

1. The design of haptic modules and mixing operators. We present six modules exerting a resistance, detent, or bounce haptic effect within a linear or rotary path and additional two ortho-planar linear bounce modules with straight and curved beams. We also propose two mixing operators for composing multiple modules: parallel mixing and series mixing.

2. Mathematical models predicting haptic properties from geometric parameters of the modules. The models adjusted from analytical theories were validated by FEA and empirical data derived from modules fabricated with the three methods.

3. Design editor. Based on the mathematical models and experiment results, FlexHaptics editor transforms haptic properties input by designers into module geometries. Moreover, the editor can adjust geometries according to selected fabrication methods to mitigate fabrication errors.

4. Six example applications. We demonstrate a broad spectrum of use cases applying the proposed techniques and tool, including two on-touchscreen interfaces of a slider control and a piano keyboard, a tactile low vision timer, VR game controllers, and a joystick combining with a two-step button.

2 RELATED WORK

We build upon prior work on constructing the design space of haptic inputs, techniques to create passive haptic inputs, and programming force-movement properties via geometric structures.

2.1 The design space of haptic inputs

Input devices transduce user movements into logical values of an application [7], and haptic devices provide haptic feedback in response to user movements [11]. Thus we identify the design space of haptic inputs consists of two dimensions: movement path and haptic effect. *Card et al.* [7] propose that possible movement paths of input devices can be described with primitive movements (i.e., linear and rotary) and operators (i.e., merge, layout, and connect) to combine the primitives. Thus inspired, FlexHaptics modules support linear and rotary paths and combine for complex paths.

Among various haptic effects [17], we narrow our scope down to passive force-movement properties, which is commonly visualized as a curve about forces against displacement. Varying force intensity and direction (assisting or resisting movement) along a

path generates numerous patterns of communicating value. Researchers have facilitated the design force-movement patterns on active hardware with editors, APIs, or codes that provide useful and frequent patterns, including barrier, spring, friction, damper, and acceleration [18, 24, 36, 37, 39]. For passive haptic interfaces, while some efforts support freely composing force-movement patterns [20], most efforts provide a set of mechanisms, each of which exerts a typical pattern. Moreover, *Mechamagnets* [41] proposes six haptic profiles by magnets configurations, which can cross with five spatial constraints by 3D-printed widgets to extend possibilities. Our method covers the commonly used force-movement patterns (friction/resistance, detent, spring/bounce) and allows stacking the patterns on a movement path (by parallel mixing). And we adapt *Mechamagnets*'s [41] idea of separating and crossing the haptics and movements to expand coverage over the design space.

2.2 Techniques to create passive haptic inputs

Several techniques to create passive haptic inputs leverage magnetic materials. The techniques require manual process, like embedding permanent magnets in *Mechamagnets* [41] and *Magneto-haptics* [20] and rubbing magnetic rubber sheets with a magnetizing tool in textitMagnetact [40]. While these techniques are easy to craft, the predetermined magnetic materials may limit fine-tuning haptic properties.

Elastic materials bring tangible inputs with flexibility without complicating their mechanical structures. For instance, *Rivera et al.* [25] present input devices made by embedding elastic textile between rigid part during 3D-printing. Moreover, the emergence of flexible-material 3D printing makes the fabrication more automated. For example, *Flexibles* [31] leverages TPU filaments and *Slyper and Hodglns* [34] use rubber-like material for 3D-print flexible mechanisms.

Origami and kirigami-based techniques use computation for designing cut-and-fold patterns and employing widely accessible machines and materials for fabrication, as demonstrated by *Foldio* [21] and *Sensing kirigami* [42]. Recently, *Kirigami Haptic Swatches* [8] has enabled designers to quantitatively adjust the force feedbacks of four types of kirigami buttons based on mathematical models linking force feedbacks to geometric parameters and laser cutting settings.

Researchers have demonstrated techniques to program the flexibility of an object 3D-printed from a single and relatively stiff material by adjusting the structure geometries. For instance, *Panetta et al.* [22], *Schumacher et al.* [32], and *Ion et al.* [14] present metamaterial methods that arrange microstructures at different flexibility to control the elasticity distributions of assemblies. *Ondulé* [12] leverages coil spring structures, complemented with mechanical joints, to control bounce effects along various movement paths. Like ours, these methods use widely available 2D-cutting or 3D-printing machines and a single regular material and allow quantitative control over force-movement patterns. However, the micro-scale and coil structures are less fabricable when scaled down to small sizes needed by finger-scale inputs (e.g., keyboard). In contrast, our method leverages simpler cantilever structures to support compact input designs.

2.3 Structural flexibility design and fabrication

A beam is a slender structural element to resist load, commonly used in machine design. Cantilever beams, beams supported on only one end, contribute to tactile feedback in many daily products, like snap-fit mechanisms and detent mechanisms [4]. *Rizescu et al.* [26] and *Ji et al.* [15] investigate the effects of topologies on tactile sensations of cantilever snap-fit mechanisms. Mechanical simplicity makes beams suitable for digital design and fabrication. For example, *Lamello* [30] leverages comb-like structure with varying-length tines in 3D-printed input interfaces. *Roumen et al.* [29] apply straight and curved cantilevers for robust joints and mounts in laser-cut products. *Klahn et al.* [16] and *Robeller et al.* [27] provide guidelines for 3D printing or CNC fabricating snap-fits. Moreover, reaction forces from deflected beams can be calculated with analytical methods based on, e.g., Euler-Bernoulli theory [2] and Castigliano's theorem [9]. The design of FlexHaptics modules incorporate findings from these efforts to ensure the modules provide proper haptic sensations, are reliable to fabricate, and can be precisely calculated.

3 FLEXHAPTICS

3.1 Design Goals

Our design goals for FlexHaptics modules are as follows:

Functional. We ensured a module constrained movement within a path and generated force feedback as designed. We also enabled each module design to provide a proper range of force feedback. For instance, we broadened that of resistance modules by setting not only beam length but also beam width and thickness as variables. Moreover, we made sure that designers could adjust each haptic feature without influencing the others in a module. For example, to allow independent adjustment of stiffness and linear-stiffness range in a linear bounce module, we set not only beam length and unit number but also beam thickness and width as variables because decreasing the former two increases stiffness but shortens linear range and adjusting later two can correct the side effect.

Compact. As many devices are compact colligation of simple inputs (e.g., keyboard), we recognized compactness is critical for the modules to be widely applicable. We simplified geometries so that they can function when scaled down to the fingertip size. We minimized extra space by shaping beams according to operating areas, such as rotary resistance and ortho-planar bounce modules.

Easy to fabricate. We recognized challenges in using consumer-grade machines to fabricate parts with thin and slender features, as well as in assembling tiny parts. Thus we minimized such features and part numbers. We included three fabrication methods, including 1) laser cutting acetal plastic (POM) sheet, 2) laser cutting extruded acrylic sheet, and 3) 3D printing PLA filament, to allow designers choices regarding tool accessibility and design requirement. We selected the materials for two reasons. First, they are easy to fabricate using widely-available machines such as laser cutters and 3D printers. Second, the materials are strong, yet flexible indicated by high ratios of strength to Young's modulus [13]. Delrin has a better ratio, while transparent acrylic is useful to on-touchscreen see-through interfaces.

Predictable. We aimed for that force feedback generated by a module design could be precisely predicted. As our module designs

and mathematical models are based on existing analytical models, we made sure the conditions for the formulas were met. For instance, the linear resistance module is based on Euler-Bernoulli's theory calculating the reaction force of a beam with its geometry and end deflection when the deflection is small [2]. Therefore, we applied a wedge cut between the tip and beam to minimize the tip's effect on the beam geometry. And we adapted a circular tip so that the deflection of a beam end (the circle center) would always equal to tip radius regardless of beam bending degree. And we maintained the tip radius less than 1/10 of the beam length to meet the small deflection condition.

3.2 Overview of modules and mixing operators

FlexHaptics approaches haptic input design by parameterizing two attributes: the movement path and the haptic effect. The movement path includes linear and rotary motions, and the haptic effect comprises resistance, detent, and bounce feedback patterns. As shown in Figure 3, resistance refers to a force with a steady magnitude and a direction opposite to movement, detent refers a force-displacement pattern where resistance increase and decrease within a short displacement, and bounce refers to a resisting force that decreases or increases as displacement decreases or increases.

By crossing the movement paths and haptic effects, FlexHaptics provides eight primitive modules, each of which supports a haptic effect along a movement path. The modules include linear resistance, linear detent, linear bounce, rotary resistance, rotary detent, and rotary bounce modules (Figure 3), and additionally, an ortho-planar linear bounce module that generates a bounce effect along an out-of-plane linear movement path and a planar bounce module whose mobile part moves free on the plane and exerts bounce effect.

Multiple modules can be combined into composite inputs through two mixing strategies: mixing in parallel and mixing in series (Figure 4). Mixing in parallel aligns and respectively bonds the mobile and static parts of two or more modules with the same movement path, producing a compound input with multiple haptic effects along the single path. Mixing in series bonds the base of one module or composite input to the mobile part of another, so on and so forth. The resulted inputs have a complex movement path and maintain component haptic effect(s) along each component path.

3.3 Module Design

This section introduces each module design, focusing on the prediction of haptic property from the geometric parameters. The predictions are embodied in linear regression equations (see Eq. 1,4, 11, 15,16), which constitute a compound explanatory variable containing multiple geometric parameters, **coefficient (A)**, and **constant (B)**. This section describes the explanatory variables that are determined by adjusting existing analytical models of beams according to our module designs. **As and Bs accommodate flexibility caused by the rest part of a module except the beam and material effects**. Such predictions avoid using material property measures (e.g., Young's modulus, Poisson's ratio), which are hard to decide for fabricated parts since they are affected by laser cutting or 3D printing process. **As and Bs' calculations and values are present in Section 4**.

3.3.1 Resistance feedback. A resistance module consists of a deformable mobile part squeezed into and moving along a linear or rotary track. The raised-end cantilever embedded in the mobile part deflects and exerts a reaction force, which transfers to sliding or rotating resistance between the two parts with a certain friction coefficient.

Linear resistance modules. A linear resistance module provides a constant force resistant to sliding (Figure 5). The deformed beam yields a reaction force F_{LR-r} predictable with l , b , h , and free end displacement when displacement is small according to Euler-Bernoulli theory [2], and displacement equals r_t (Eq. 1). Normal force N between the two parts can be calculated from the reaction force, according to the mechanical equilibrium equations of the tip and slider (Eq. 2). Force feedback of a linear resistant module F_{LR} equals the sum of sliding resistance, which is the product of normal force and friction coefficient μ decided by material property (Eq. 3). In summary, force feedback from a linear resistance module of certain material is predictable from the module geometry, as shown by substituting Eq. 1 and 2 into 3.

$$F_{LR-r} = A \frac{r_t b h^3}{l^3} + B \quad (1)$$

$$N = 2F_{LR-r} \quad (2)$$

$$F_{LR} = \mu N \quad (3)$$

Rotary resistance modules. A rotary resistance module provides a constant torque resistant to rotating (Figure 6). The deformed beam exerts a reaction force predictable with r , a , b , h , and displacement according to Castigliano's theorem [9], and displacement equals r_t (Eq. 4). Normal force between the two parts can be calculated from the reaction force, according to the mechanical equilibrium equations of the tip and rotor (Eq. 5). Feedback torque of a rotary resistant module T_{RR} equals the sum of resistant torque, which is the product of normal force, friction coefficient, and R (Eq. 5). In summary, the feedback torque from a rotary resistance module on certain material is predictable from the module geometry and material, as shown by substituting Eq. 4 and 5 into 6.

$$F_{RR-r} = A \frac{r_t b h^3}{r^3 (2a - \sin 2a)} + B \quad (4)$$

$$N = 2F_{RR-r} \quad (5)$$

$$T_{RR} = \mu N R \quad (6)$$

3.3.2 Detent feedback. A detent module consists of a mobile part moving along a linear or rotary track with notches (Figure 7). The mobile parts employ the same beam structure of linear resistance modules, which has a raised tip conforming to the notches. Friction between a mobile part and track is removed by adding lubricant, and force feedback of sliding or rotating equals the tangential component of normal force between the two parts.

Given the geometry of a detent module, what is known is the notch profile $y = f(x)$, where x and y are the horizontal and vertical position of a point on the notch, the notch slope is $f'(x)$, and the beam stiffness k predictable from b , l , and h (Eq.1), and tip radius r_t .

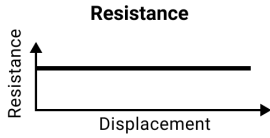
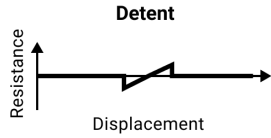
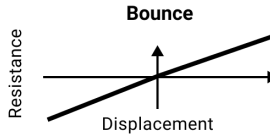
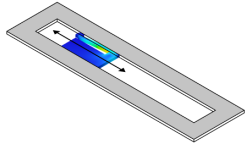
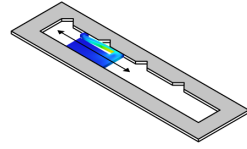
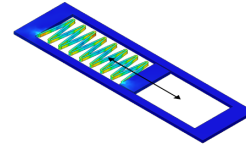
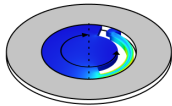
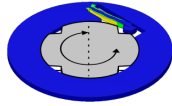
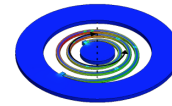
		Haptic Effect			
		Resistance	Detent	Bounce	
					
Movement Path	Linear				Ortho-planar
	Rotary				

Figure 3: FlexHaptics modules. A FlexHaptics module supports a haptic effect among resistance, detent, and bounce, along a linear or rotary path. The left six modules afford within-plane path, the two additional modules are designed for bounce effect along an out-of-plane linear path. Gray parts are rigid; colored parts are compliant, and color changing from blue to green, and to red indicates increasing stress levels.

What can be calculated is beam deflection δ (Eq.7 or 8) and reaction force (Eq.9) when the beam moving along the notch. And the force feedback during the movement is the horizontal component of the reaction force (Eq.10).

When contact point is derivable (Figure 7 A right),

$$\delta = \sqrt{r_t^2 - x^2} \quad (7)$$

When contact point is not derivable (Figure 7 A left),

$$\delta = \text{tr} \left(1 - \frac{1}{\sqrt{1 + f'(x)^2}} \right) - f(x) \quad (8)$$

$$F_{D-r} = k\delta \quad (9)$$

$$F_D = F_{D-r} f'(x) \quad (10)$$

Various detent effects can be designed by adjusting notch profiles, beam geometries, and notch distributions. A notch profile can be created by selecting a left side and a right side from the four preset notch profiles: 1) constant slope, 2) increasing slope, 3) increasing then decreasing slope, 4) locking. A notch can be scaled along or perpendicular to the movement direction, influencing the detent effect scope and sharpness. Adjusting the beam increase or decrease force feedback along the notch consistently.

3.3.3 Bounce feedback. Bounce modules exert a restoring force (F) toward the equilibrium and proportional to displacement when the mobile part is moved away from the neutral position within a range. Bounce coefficients can be adjusted by altering geometric parameters.

Linear bounce module. A linear bounce module provides a resistance force that is proportional to displacement when stretched

or squeezed within a range (Figure 8). A linear bounce module is constructed with a series of beams. The bounce coefficient $k_{LB\text{-unit}}$ of each unit can be predicted with l , b , and h (Eq.10), and that of whole module k_{LB} can be further calculated with the number of units based on series spring formulas (Eq.11).

$$k_{LB\text{-unit}} = A \frac{bh^3}{l^3} + B \quad (11)$$

$$k_{LB} = \frac{k_{LB\text{-unit}}}{n} \quad (12)$$

Rotary bounce module. A rotary bounce module allows the arbor to rotate and exerts reaction torque proportional to the rotating angle (Figure 9). The design of the spring was based on the standard Archimedean spiral defined by da , h , p , and a , from which its effective length l can be calculated (Eq.13, 14, and 15) [3]. And the bounce coefficient can be calculated with b , h , and l according to spiral spring theory (Eq.16) [3].

$$l = -\frac{1}{2y} \left[x\sqrt{x^2 + y^2} + y^2 \ln \left(x + \sqrt{x^2 + y^2} \right) - (x + ya)\sqrt{x^2 + y^2 + 2xya + y^2 a^2} - y^2 \ln \left(x^2 + y^2 + 2xya + b^2 a^2 \right) \right] \quad (13)$$

$$x = \frac{da + h}{2}, \text{ where } d = 10 \quad (14)$$

$$y = \frac{p}{2\pi}, \text{ where } p = 2h \quad (15)$$

$$k_{RB} = A \frac{bh^3}{l} + B \quad (16)$$

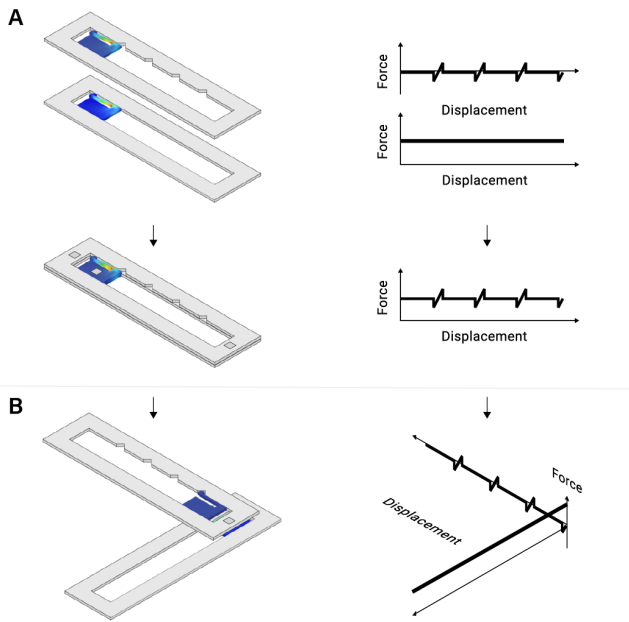


Figure 4: Two mixing operators for FlexHaptics modules. (A) Mixing in parallel aligns modules with the same movement path and bonds the mobile and static parts together respectively, resulting in an interface with the same movement path and a compound haptic effect. (B) Mixing in series uses multiple modules with different movement paths, and bonds the static part of one module to the mobile part of another module, producing an interface with a complex movement path.

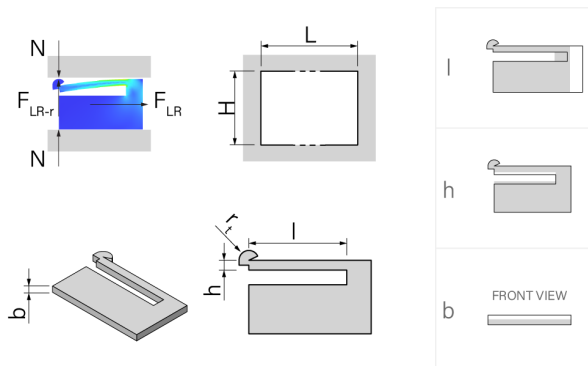


Figure 5: Linear resistance module. It comprises a flexure slidable along a linear track. Its force feedback is adjusted with beam length l , thickness h , and width b .

Ortho-planar linear bounce modules. Ortho-planar linear bounce modules provide the mobile platform moving out of the base plane with a resistance force proportional to displacement (Figure 10 and 11). They are constructed with a straight or round beam following the mobile platform shape. Bounce coefficients of straight beams can be calculated with l , b , h [2]. Bounce coefficient

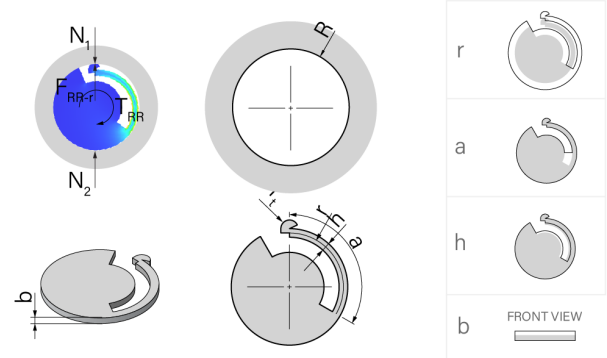


Figure 6: Rotary resistance module. It consists of a flexure rotatable within a ring. Its force feedback is adjusted with beam radius a , radius r , thickness h , and width b .

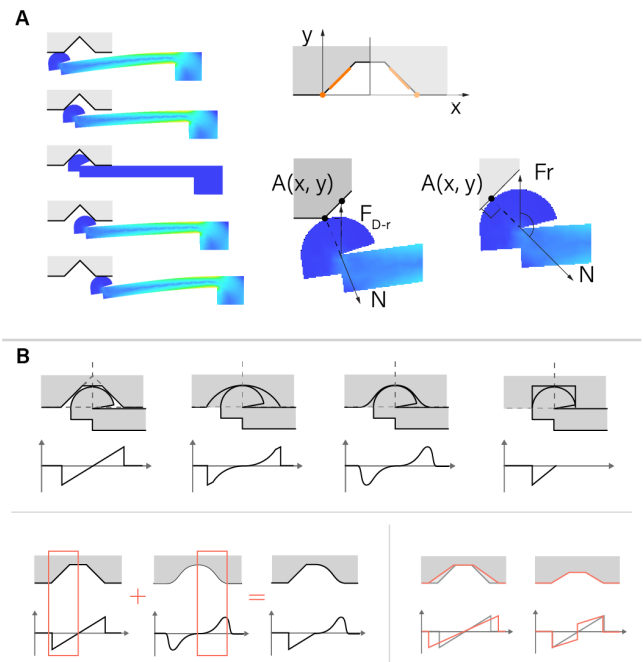


Figure 7: Detent modules. A linear and rotary detent module both employ the same beam geometries as linear resistance module and adapts notches to contact surface. (A) As the beam moving across a notch, force feedback is determined by the notch and beam geometry. (B) We present four symmetrical notch signatures and force-displacement curves. Mixing a left and a right side of them generates another 12 detent profiles. Force feedback from a notch can be adjusted by scaling it along its width or depth direction.

of round beams can be predicted with l (i.e., a and r), b , h based on [19].

$$k_{OLBS} = A \frac{bh^3}{l^3} + B \quad (17)$$

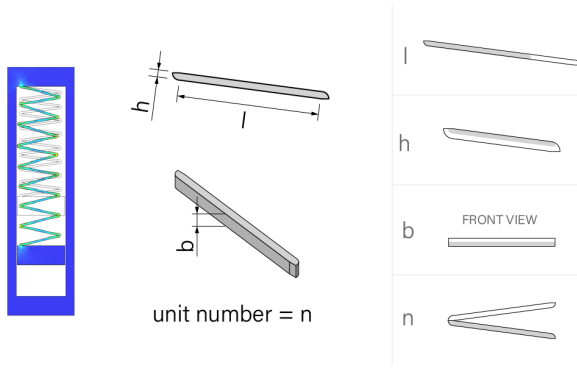


Figure 8: A linear bounce module can be stretched or compressed, its stiffness can be adjusted by beam length l , thickness h , and width b , and unit number n .

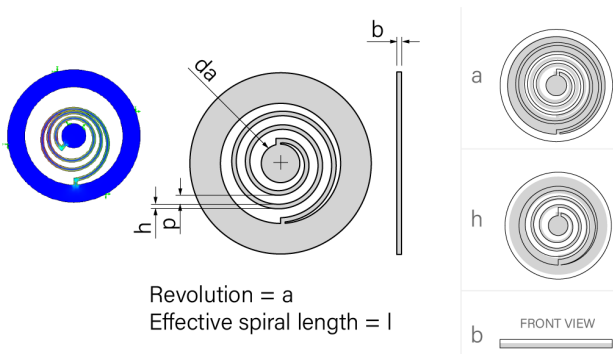


Figure 9: A rotary bounce module can be rotated clockwise or counterclockwise, its stiffness can be adjusted by spiral radian a and wire thickness h and width b .

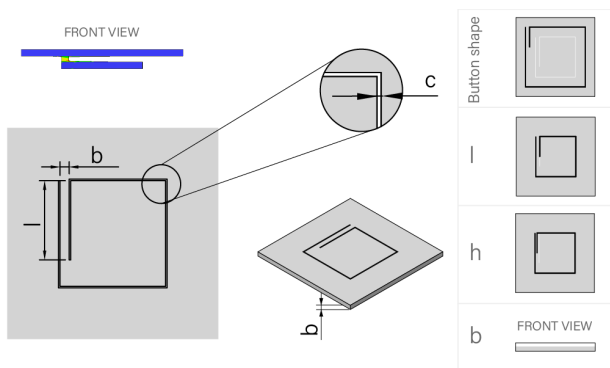


Figure 10: A straight-beam ortho-planar bounce module can be adjusted with beam length l , thickness h and width b .

$$k_{OLBR} = A \frac{bh^3}{(ra)^3} + B \quad (18)$$

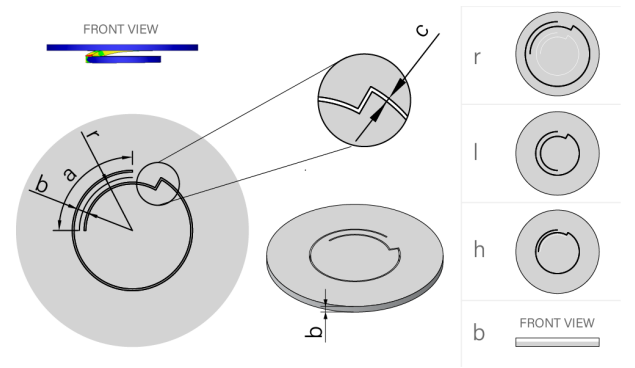


Figure 11: A curve-beam ortho-planar bounce module can be adjusted with beam radius r , radian a , and beam thickness h and width b .

4 TECHNICAL EVALUATION

We evaluated how well the mathematical models predict modules of FEA simulation and modules fabricated with the three methods. FEA simulation allowed investigating ideal modules that the sizes are precise and the material properties are the same as provided by the manufactures. Experiments were for identifying effects from fabrications, informing adjustments to FlexHaptics techniques.

4.1 Fabrication methods and testing settings

We fabricated modules of different materials using machine settings (Table 1) that balance fabricating quality and time. Moreover, we adjust digital models in response to fabrication errors and fit clearances. To adjust laser cutting errors, we flipped one part of a module in to improve incorporations between parts, addressing slanted kerf [28], and offset laser cutting profiles 1mm outer to mitigate material removed by cutting. For 3D printing, we chamfered the bottom edges at 0.3mm to mitigate "Elephant's foot" where a first layer flaring outside. We maintained fit clearances for sliding and rotating fit of different materials when there is minimal friction and an invisible gap between two parts.

Our experiment settings consist of a console and four replaceable accessories (Figure 12). The console measure forces with a force gauge and linear displacements with a potentiometer. The four accessories connected to the console are for measuring linear reaction force, linear resistance, rotary reaction torque, and rotary resistance.

4.2 Data collection and analysis

We simulated and measured reaction force of resistance modules and stiffness of detent and bounce modules with varying geometric parameters (Table 2). Linear regression analysis was conducted to predict F_{LR-T} with $\frac{bh^3}{l^3}$ for evaluating Eq. 1, T_{RR-r} with $\frac{r_1bh^3}{r^3(2a-\sin 2a)}$ for Eq. 1, $k_{LB-unit}$ with $\frac{bh^3}{l^3}$ for Eq. 1, k_{OLBS} with $\frac{bh^3}{l^3}$ for Eq. 1, k_{OLBR} with $\frac{bh^3}{(ra)^3}$ for Eq. 1, k_{RB} with $\frac{bh^3}{l^3}$ for Eq. 1, where l is calculated from a and h . Table 3 lists coefficients and R-squared's. Finally for each module, we compared the measured curve with the curve predicted with the equations.


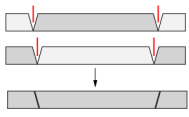


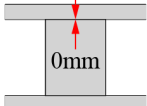
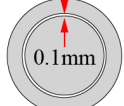
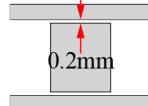
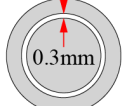
	Laser-cut POM	Laser-cut Acrylic	3D-printed PLA	
Material	Delrin 1/16"	Cast acrylic 1/16"	Ultimaker PLA	
Machine	Universal Laser Systems PLS6.150D		Ultimaker 3 and S5	
Setting	Power 15, speed 4, pass 2	Power 10, speed 8, pass 3	Profiles 0.1, infill 100%	
Adjustments	1. Outer offset 0.1mm	2. Flip one part to assemble	1. Chamfer 0.3mm	2. Align print path to beam length
				
Fit clearance	Sliding  0mm	Rotating  0.1mm	Sliding  0.2mm	Rotating  0.3mm

Table 1: Fabrication material and methods.

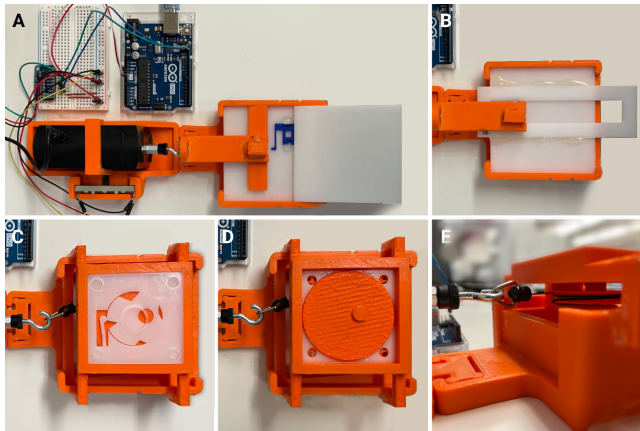


Figure 12: Experiment settings: (A) testing console and accessory for linear reaction force, (B) accessory for linear resistance, (C) accessory for rotary resistance, (D) accessory for rotary reaction force, and (E) winding mechanism for rotary modules.

4.3 Results and adjustments

Results of the linear regression analysis are shown in Table 3. The prediction method predicted the reaction force or stiffness of FEA modules with high goodness-of-fit (averaged $R^2 = 0.99836$), and fabricated modules with less goodness-of-fit (averaged $R^2_{\text{Delrin}} = 0.95341$, averaged $R^2_{\text{acrylic}} = 0.79088$, averaged $R^2_{\text{PLA}} = 0.97723$). We suppose this was because fabrication introduces dimensional errors and changes material properties. Dimensional preciseness is important to the prediction precision, for example, if h changes from 1mm to 1.1mm, the haptic values will increase changes 33.1%. 3D printing and laser cutting fabricate the same file into results different in dimensions, even with the same machines and settings. The theoretical basis of the mathematical models relies on isotropic materials. Heat in laser-cutting processes changes the flexibility of

material close to cuts, and FDM 3D printed objects have different stiffness along different directions.

Besides reactions from the beams, force feedbacks of a module was affected by other factors like friction and track stiffness. Resistance modules involved more uncertainty of force feedback because they leverage friction. First, friction coefficients were not consistent due to fabrication and contact conditions. Second, static friction was greater than kinetic friction, thus force feedback at the right beginning of a movement was greater than that during movement. For linear resistance and detent modules with a long travel distance, their tracks got less stiff, reducing the deflection of the beam and force intensities. We identified four approaches to avoid or mitigate the errors. The first is to avoid setting small values of h and b . The second is to prioritize adjusting l values instead of b or h to meet haptic values. The third is to fabricate a series of models with l values varying around the value calculated for a desired force or stiffness value so that one of the prototypes can provide the desired haptics. Lastly, we note to avoid using acrylic for linear bounce modules because of the high risk of fracture.

5 FLEXHAPTICS EDITOR

We present an editor¹ to make FlexHaptics technique available to designers. The following section introduces its interfaces and implementation.

User interface. To generate a module in FlexHaptics editor (Figure 13), designers need to go through the following steps:

- (1) Choose a module type.
- (2) Select a fabrication method and material.
- (3) Set desired haptic values. The editor generates geometry in Rhinoceros viewport and calculates its force-feedback with error range.
- (4) Explore other possible geometries. Because the same force feedback can be produced by different parameter combinations, this step allows designers to adjust a module freely

¹This editor was developed as a plugin for Rhinoceros 6 and Grasshopper for generating FlexHaptics modules. It can be accessed at <https://github.com/hlin0101/FlexHaptics>.

Module & Parameters	FEA	POM/Acylic	PLA
Linear resistance			
l	10 to 30, interval of 2		
b	1, 1.5875, 2, 3	1.5875	1,2,3
h	1, 1.5, 2, 3		
Rotary resistance			
a	60 to 120 degrees, with interval of 5		
r	7.5, 10, 15		
b	1, 1.5875, 2, 3	1.5875	1,2,3
h	1, 1.5, 2, 3		
Detent			
l	10 to 30, interval of 2		
b	1, 1.5875, 2, 3	1.5875	1,2,3
h	1, 1.5, 2, 3		
Linear bounce			
l	10 to 30, interval of 2		
b	1, 1.5875, 2, 3	1.5875	1,2,3
h	1, 1.5, 2, 3		
n	1, 2, 4, 8		
Rotary bounce			
a	90 to 1260, interval of 90		
b	1, 1.5875, 2, 3	1.5875	1,2,3
h	1, 1.5, 2, 3		
Ortho-planar linear bounce straight			
l	10 to 30, interval of 2		
b	1, 1.5, 2, 3		
h	1, 1.5875, 2, 3	1.5875	1,2,3
Ortho-planar linear bounce round			
a	60 to 120, with interval of 5		
r	7.5, 10, 15		
b	1, 1.5, 2, 3		
h	1, 1.5875, 2, 3	1.5875	1,2,3

unit for l, b, h, r is mm, a is degree

Table 2: The parameter set used to generate modules for technical evaluation. Values of a parameter are presented once in a middle cell under POM/Acrylic, if the parameter was varied by the same values across different materials.

while comparing its force-feedback in comparison to that set in Step 3.

(5) Export a final design in STL or SVG format.

Implementation. The backend of FlexHaptics editor is implemented with Grasshopper and Rhinocommon in C# and the front-end interface is developed using Human UI. In Step 4, given geometric parameters, haptic values are calculated by using the equations in the presented order. Here we present how the equations are utilized to generate modules from haptic values. For instance, linear resistance module, on receiving user input haptic value in Step 3 the algorithm first calculate the reaction force with corresponding equations (Eq 2 and 3). Then to calculate geometries from reaction force with Equation 1, the algorithm starts by setting b and h at the smallest value to calculated l , then examine if l is at least ten times as long as r_t (to meet small deformation condition). If not, the algorithm will increase h and b step by step and repeat calculating

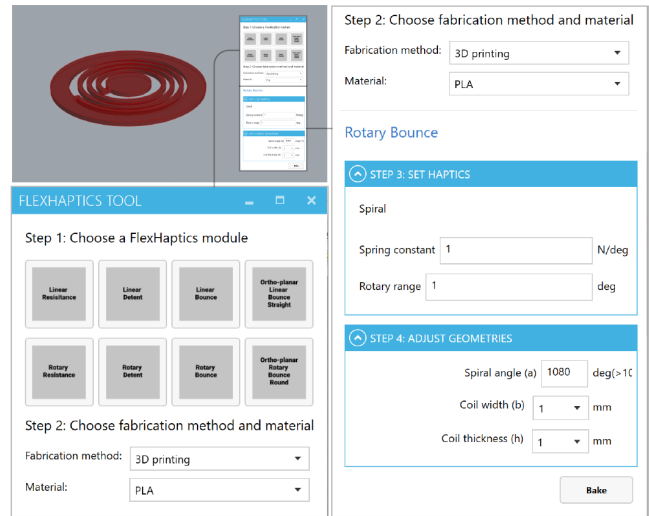


Figure 13: FlexHaptics user interface consists of a FlexHaptics tool panel and module preview in Rhinoceros environment.

and evaluating l . If yes, the algorithm will use the values to generate a geometry. Similar process applies to the other modules, Table 4 lists the parameters with default values, the parameter to calculate, and the examined condition of reach module. Once deciding on the compliant part geometry, the algorithm will adjust the other component for the two-part modules to maintain a fit clearance, and can offset the geometries for laser cutting and chamfered for 3D-printing according to Table 1.

6 APPLICATION EXAMPLES

To validate the proposed technique, we developed six example applications (Figure 14) that cover different modules, mixing operators, and fabrication methods and materials. Once deciding on a design idea, we developed the interface through the following process:

- (1) decide needed modules and their fabrication methods and materials, sizes, and haptic parameters;
- (2) use the editor to generate the modules;
- (3) model other parts of the interface with reference to the generated modules;
- (4) fabricate the components using the decided fabrication methods and materials;
- (5) assemble the components (with electrical elements if needed), test, and iterate.

Below we present them in three categories according to application environments.

6.1 Haptic layers above graphics on touchscreens

We demonstrate two examples made by laser-cutting acrylic sheets and attaching copper tapes to align with graphics and transit user touches on touchscreens.

Module & Equation	FEA (POM)			POM			Acrylic			PLA		
	A	B	R ²	A	B	R ²	A	B	R ²	A	B	R ²
Linear resistance												
h=1, 1.5	1312.3	0.0033	0.9999	1493.6	0.0377	0.818	1438.8	0.1249	0.2115	1982.2	0.0051	0.9981
h=2	1117.3	0.0708	0.9996	1481.6	-0.0161	0.9926	1235.5	0.0305	0.9657	1497.3	0.3891	0.9393
h=3	880.4	0.3673	0.9993	1170.6	0.3049	0.9926	910.91	0.6316	0.8522	1083	0.7627	0.9991
Rotary resistance												
	1480.1	0.0672	0.9997	1450.1	0.9677	0.9677	1191.7	0.653	0.9619	1822.5	0.6443	0.9391
Detent												
h=1, 1.5	656.15	0.0017	0.9999	746.8	0.0189	0.818	719.4	0.0625	0.2115	991.1	0.0026	0.9981
h=2	558.65	0.0354	0.9996	740.8	-0.0081	0.9926	617.75	0.0153	0.9657	748.65	0.1946	0.9393
h=3	440.2	0.1837	0.9993	585.3	0.1525	0.9926	455.46	0.3158	0.8522	541.5	0.3814	0.9991
Linear bounce												
	1732.2	0.2977	0.9929	2616.6	0.2244	0.9706	1893.6	0.3796	0.9563	2180.2	0.8661	0.9691
Rotary bounce												
	205.36	0.0058	0.9082	214.19	0.083	0.8828	189.23	0.0622	0.9065	275.76	0.054	0.903
Ortho-planar bounce round												
	776.77	0.0569	0.9934	960.4	0.0492	0.9896	911.42	-0.0969	0.9322	1019.8	-0.0266	0.9924
Ortho-planar bounce straight												
	794.14	0.0051	1	1086.9	0.0035	0.9998	865.44	0.0101	0.9996	1166	0.0359	0.9987

Table 3: Results of linear regression analysis.

Module	Adjustable by users		Generated by algorithm		
	Step 2	Step 4	Preset	Calculated	Condition
Linear resistance	Resistance force	l, b, h	b, h	l	l > 10 tr
Rotary resistance	Resistance force	a, r, b, h	b, h, r	a	a * r > 10 * tr
Linear detent	Notch, k	l, b, h	b, h	l	l > 10 * tr
Rotary detent	Notch, k	l, b, h, r	b, h	l	l > 10 * tr
Linear bounce	k, range	l, b, h, n	b, h, n	l	l * n > 10 * range
Rotary bounce	k, range	da, b, h, a	b, h, da	a	a > 10 * rotary range
Ortho-planar bounce straight	k, range	l, b, h	b, h	l	l * n > 10 * range
Ortho-planar bounce round	k, range	a, r, b, h	b, h, r	l	a * r > 10 * range

Table 4: Parameters of each module. The adjustable by users in Step 3 are haptic parameters set by designers for algorithm. The adjustable by users in Step 4 are geometric parameters that designers can modify on an algorithm-generated module geometry. The generated by algorithm are geometric parameters computed by algorithm based on designers' inputs in Step 3.

Haptic control panel for a painting application. The haptic control panel for a painting application, Procreate, is proposed to reduce divided attention caused between canvas and toolbar (Figure 14 A). The transparent haptic layer overlaid on the graphical interface employs a linear resistance module for changing brush size and a linear detent module notched at preferred values for adjusting opacity. Knobs inserted into the sliders are wrapped by copper tapes to transmit user touches to a touchscreen.

Piano keyboard. We demonstrate a piano keyboard interface for a touchscreen music app (Figure 14 B) to improve user performance. Similarly, the keyboard is made from an acrylic sheet and copper tapes going around each key. We highlight that ortho-planar linear bounce modules can resemble such keyboards by being shaped and collocated.

6.2 Passive haptic proxies in VR

When using passive props for VR interaction, a key could be to use less physical materials to simulate more virtual objects. FlexHaptics could be a solution because its compactness increases the number of proxies containable within a reasonable space. We demonstrate such applications with two examples implemented with Oculus Quest and Unity 3D.

VR controller attachment for bow-shooting games. This VR controller attachment system for bow-shooting games (Figure 14 C). To use a virtual bow, players choose a proxy at the preferred level of resistance, simply plug its base end to the socket on one controller, and draw or release the free end with the other controller. A bow proxy consisting of a laser-cut POM linear bounce module sandwiched by acrylic faces simulates increasing resistance while opening a bow and retracting effects while releasing an arrow. The



Figure 14: Application examples: (A) a slider input interface for touchscreen painting applications, (B) a piano keyboard interface for touchscreen musical applications, (C) a VR controller attachment for bow shooting games, (D) a string-based wearable haptic device, (E) a tactile low vision timer, and (F) a joystick with a two-step button on the stick end.

position and orientation of a proxy can be drawn from those of the associated controller.

String-based wearable haptic device. We demonstrate a haptic device worn between wrist and fingertips, which provides haptic feedback to different gesture interactions in VR (Figure 14 D). This design is inspired by FlexiFingers that is mounted on the wrist and provides fingers with passive forces or constraints[1], as well as Wireality that delivers haptic effects to hand joints with retractable strings [10]. Our device comprises multiple stackable string-retracting units, each of which leverages a rotary bounce module for retracting and another rotary module for more haptic effects. We made the modules by 3D-printing PLA, as its easier to integrate other extruded structures, like bobbins and tongue joints. Thanks to the compact form factors of the FlexHaptics modules, a stack of three units is as small as a smartwatch.

6.3 Haptic controls with microcontrollers

The following examples present FlexHaptics interfaces embedded with circuits and connected to microcontrollers. Drawing on research and projects on paper circuits, we built most circuits² with copper tapes, conductive ink, manually or using a cutting machine. We note potential alternative methods, including 3D-printing [6, 38], screen printing, and inkjet printing with functional filaments or inks.

Tactile timer input. We present a tactile timer input for low-vision people (Figure 14 E). Each dial consists of a rotary resistance and detent module. The hour, minute, and second dials present diminishing resistances and different detent densities. Starting and canceling buttons are made with ortho-planar modules. We made the input by 3D-printing PLA, as it is easier to integrate extruded

²Paper circuit patterns can be accessed at <https://github.com/hlin0101/FlexHaptics>.

knobs and marks. This prototype highlights a compact design enabled by nesting the three dials in the same layer.

Haptic controls with complex movement paths. The joystick designed for a shooting game can control shooting direction and switch between single or scattering shots (Figure 14 F). It allows rotation in horizontal and vertical planes by serial-mixing two mutually perpendicular rotary bounce modules. The button on the handle can activate single or scattering shooting mode under light or hard press. It employs in-series mixing two ortho-planar bounce modules with different bounce constants. **The modules are made by laser-cutting POM sheets.** This example demonstrates composing a complex 3D movement path by mixing modules in different planes.

7 LIMITATIONS & FUTURE WORK

As we acknowledge several limitations of the FlexHaptics, we propose future work to address the issues.

Fabrication error, material fatigue and creep, external friction. The current mathematical models are limited due to three causes of differences between actual and predicted haptic effects of the FlexHaptics interface. **The first is fabrication errors, as indicated by the less goodness of fit for the fabricated modules.** Designers can make up by making a range of models containing a desired one, as described in Section 4.3. **The second is material fatigue and creep, as with the majority of techniques. Detent and bounce modules in interaction are under cyclic loading, thus will get weaker after extensive use. Resistance and detent modules are influenced by persistent mechanical stresses even not in usage, thus will exhibit dimmer haptic effects after a long term of preservation. Designers need to replace exceedingly used or old ones to maintain haptic preciseness. We will address the two factors by exploring more fabrication methods and materials.** Lastly, the actual haptic effects of an interface come from the modules, as well as friction between the modules and external objects (e.g., circuit layers, housing structures, or touchscreens), which is unpredictable by FlexHaptics editor. Designers can iterate modules to counteract the external friction for satisfying results. We will investigate ways to avoid external frictions, like minimizing surface areas in contact with external objects and maintaining gaps between the modules and external objects via housing structures.

Supplementary structures. The method does not assist in designing two types of supplementary structures that are often necessary in FlexHaptics interfaces. **The first type helps constrain mobile parts to designed movement paths, e.g., preventing those in resistance, detent, and linear and rotary bounce modules from moving out of tracks and guiding that in a rotary bounce module to rotary instead of translational movements.** The second is to bond parts in mixing modules or bond a module to other structures. Among tested techniques, like 3D printing different parts as one and gluing, tongue-and-hole jointing stands out as it is strong for connection and flexible for replacement. The design of supplementary structures varied to adapt to different applications. It was not very difficult but certainly complicated the overall design process. In the future, we will explore mechanisms functioning with fewer supplementary structures and have FlexHaptics editor support the generation.

Broadening materials. FlexHaptics editor now supports limited material choices. For future work, we plan to widen the available material selections based on the mathematical models. For instance, SLA resins and metals for stronger, compacter, and accurater modules. We also plan to adapt elastic materials (e.g., TPU) and even programmable filaments presented by Takahashi et al. [35] to expand the design and fabrication space of haptic input interfaces. Taking resistance modules as an example, applying multiple materials with different friction coefficients to the track boundary produces a module with varying resistance along the path. Finally, stimuli-responsive material could enable FlexHaptics modules with adaptive haptic feedback. For instance, applying stiffness-changing material to the flexures could produce modules with adaptive resistance, bounce coefficient, and detent magnitude, and using shape-changing material to the notches could produce detent modules with adaptive feedback profile and distribution.

Active force feedback and vibration feedback. **This method is limited to passive force feedback generated by the module design. Due to the passive nature, FlexHaptic interfaces cannot automatically perform tasks (like timing task in Application Example E), proactively initiate touches, or spontaneously adjust profiles. Future work could investigate ways to actuate FlexHaptics modules while maintaining their compactness, like by using smart materials.** Besides, force feedback, vibration is also important as they widely exist in natural and artificial interactions. We excel at perceiving with numerous receptors embedded in our skin and other haptic organs. Interaction with resistance and detent modules involves vibration, which can simulate human sensitivity by adjusting beam stiffness and track texture. We found it possible to introduce texture by laser-cutting a smooth line with low-power settings on extruded acrylic sheets and by designing notch profiles and distributions. We plan to add supplement vibration modules to FlexHaptics.

User-centered evaluation. We performed evaluation led by the team while developing FlexHaptics. We plan to conduct user evaluation of FlexHaptics techniques and editor to improve the system with real-world users. We will investigate whether designers can adapt and find the proposed modules and mixing operators to be useful in their design processes, and identify areas to improve further.

8 CONCLUSION

In this paper, we proposed FlexHaptics, a computational design method to create haptic input interfaces with custom feedback using a low-cost 3d printer or a laser cutter. FlexHaptics editor comprises eight primitive modules that exert a haptic effect, i.e., resistance, detent, and bounce, along a movement path, i.e., linear, rotary, ortho-planar linear, and planar. Each FlexHaptics module supports adjustable haptic effects via module geometries. Using the editor, designers can create various movement paths by customizing a module or combining multiple modules to formulate disparate haptic effects with fine-tuning. We also presented six application examples as validation of the proposed method.

Our work does not limit designers' creativity with any predefined off-the-shelf components and allow building their own devices including sophisticated haptic feedback design. Further, as haptic interface development is an iterative process of design, prototyping,

and testing, if designers make one prototype faster, the overall process accelerates exponentially. We believe FlexHaptics can be a powerful tool to create haptic input interfaces with extensive customizability and minimum manual labor.

REFERENCES

- [1] Merwan Achibet, Benoît Le Gouis, Maud Marchal, Pierre-Alexandre Leziart, Ferran Argelaguet, Adrien Girard, Anatole Lécuyer, and Hiroyuki Kajimoto. 2017. FlexiFingers: Multi-finger interaction in VR combining passive haptics and pseudo-haptics. In *2017 IEEE Symposium on 3D User Interfaces (3DUI)*. IEEE, 103–106.
- [2] Oliver A Bauchau and James I Craig. 2009. Euler-Bernoulli beam theory. In *Structural analysis*. Springer, 173–221.
- [3] VB Bhandari. 2010. *Design of machine elements*. Tata McGraw-Hill Education.
- [4] Paul R Bonenberger. 2000. *The First Snap-Fit Handbook: Creating Attachments for Plastics Parts*. Hanser.
- [5] Stefan J Breitschaft, Stella Clarke, and Claus-Christian Carbon. 2019. A theoretical framework of haptic processing in automotive user interfaces and its implications on design and engineering. *Frontiers in Psychology* 10 (2019), 1470.
- [6] Jesse Burstyn, Nicholas Fellion, Paul Strohmeier, and Roel Vertegaal. 2015. Printput: Resistive and capacitive input widgets for interactive 3D prints. In *IFIP Conference on Human-Computer Interaction*. Springer, 332–339.
- [7] Stuart K Card, Jock D Mackinlay, and George G Robertson. 1990. The design space of input devices. In *Proceedings of the SIGCHI conference on Human factors in computing systems*. 117–124.
- [8] Zekun Chang, Tung D Ta, Koya Narumi, Heeju Kim, Fuminori Okuya, Dongchi Li, Kunihiro Kato, Jie Qi, Yoshinobu Miyamoto, Kazuya Saito, and Others. 2020. Kirigami Haptic Swatches: Design Methods for Cut-and-Fold Haptic Feedback Mechanisms. In *Proceedings of the 2020 CHI Conference on Human Factors in Computing Systems*. 1–12.
- [9] Tore Dahlberg. 2004. Procedure to calculate deflections of curved beams. *International journal of engineering education* 20, 3 (2004), 503–513.
- [10] Cathy Fang, Yang Zhang, Matthew Dworman, and Chris Harrison. 2020. Wireality: Enabling Complex Tangible Geometries in Virtual Reality with Worn Multi-String Haptics. In *Proceedings of the 2020 CHI Conference on Human Factors in Computing Systems*. 1–10.
- [11] Vincent Hayward, Oliver R Astley, Manuel Cruz-Hernandez, Danny Grant, and Gabriel Robles-De-La-Torre. 2004. Haptic interfaces and devices. *Sensor review* (2004).
- [12] Liang He, Huaishu Peng, Michelle Lin, Ravikanth Konjeti, François Guimbretière, and Jon E Froehlich. 2019. Ondulé: Designing and Controlling 3D Printable Springs. In *Proceedings of the 32nd Annual ACM Symposium on User Interface Software and Technology*. 739–750.
- [13] Larry L Howell. 2013. Compliant mechanisms. In *21st century kinematics*. Springer, 189–216.
- [14] Alexandra Ion, David Lindlbauer, Philipp Herholz, Marc Alexa, and Patrick Baudisch. 2019. Understanding metamaterial mechanisms. In *Proceedings of the 2019 CHI Conference on Human Factors in Computing Systems*. 1–14.
- [15] Jingjing Ji, Kok-Meng Lee, and Shuyou Zhang. 2011. Cantilever snap-fit performance analysis for haptic evaluation. (2011).
- [16] Christoph Klahn, Daniel Singer, and Mirko Meboldt. 2016. Design guidelines for additive manufactured snap-fit joints. *Procedia Cirp* 50 (2016), 264–269.
- [17] Susan J Lederman and Roberta L Klatzky. 2009. Haptic perception: A tutorial. *Attention, Perception, & Psychophysics* 71, 7 (2009), 1439–1459.
- [18] Tania K Morimoto, Paulo Blikstein, and Allison M Okamura. 2014. [D81] Hapkit: An open-hardware haptic device for online education. In *2014 IEEE Haptics Symposium (HAPTICS)*. IEEE, 1–1.
- [19] Nam-Trung Nguyen, Thai-Quang Truong, Kok-Keong Wong, Soon-Seng Ho, and Cassandra Lee-Ngo Low. 2003. Micro check valves for integration into polymeric microfluidic devices. *Journal of Micromechanics and Microengineering* 14, 1 (2003), 69.
- [20] Masa Ogata. 2018. Magneto-haptics: Embedding magnetic force feedback for physical interactions. In *Proceedings of the 31st Annual ACM Symposium on User Interface Software and Technology*. 737–743.
- [21] Simon Olberding, Sergio Soto Ortega, Klaus Hildebrandt, and Jürgen Steimle. 2015. Foldio: Digital fabrication of interactive and shape-changing objects with foldable printed electronics. In *Proceedings of the 28th Annual ACM Symposium on User Interface Software & Technology*. 223–232.
- [22] Julian Panetta, Qingnan Zhou, Luigi Malomo, Nico Pietroni, Paolo Cignoni, and Denis Zorin. 2015. Elastic textures for additive fabrication. *ACM Transactions on Graphics (TOG)* 34, 4 (2015), 1–12.
- [23] Pornthep Preechayasomboon and Ali Israr. 2020. Crossing the Chasm: Linking with the Virtual World through a Compact Haptic Actuator. In *Extended Abstracts of the 2020 CHI Conference on Human Factors in Computing Systems*. 1–4.
- [24] Pornthep Preechayasomboon, Ali Israr, and Majed Samad. 2020. Chasm: A Screw Based Expressive Compact Haptic Actuator. In *Proceedings of the 2020 CHI Conference on Human Factors in Computing Systems*. 1–13.
- [25] Michael L Rivera, Melissa Moukperian, Daniel Ashbrook, Jennifer Mankoff, and Scott E Hudson. 2017. Stretching the bounds of 3D printing with embedded textiles. In *Proceedings of the 2017 CHI Conference on Human Factors in Computing Systems*. 497–508.
- [26] Ciprian Ion Rizescu and Dana Rizescu. 2020. Mechanical Behaviour Analysis of Snap Joints for Haptic Evaluation. In *International Conference of Mechatronics and Cyber-Mixmechatronics*. Springer, 12–19.
- [27] Christopher Robeller, Paul Mayencourt, and Yves Weinand. 2014. Snap-fit joints-CNC fabricated, integrated mechanical attachment for structural wood panels. In *ACADIA 2014 Design Agency: Proceedings of the 34th Annual Conference of the Association for Computer Aided Design in Architecture*. Riverside Architectural Press, 189–198.
- [28] Thijs Roumen, Ingo Apel, Jotaro Shigeyama, Abdullah Muhammad, and Patrick Baudisch. 2020. Kerf-canceling mechanisms: making laser-cut mechanisms operate across different laser cutters. In *Proceedings of the 33rd Annual ACM Symposium on User Interface Software and Technology*. 293–303.
- [29] Thijs Roumen, Jotaro Shigeyama, Julius Cosmo Romeo Rudolph, Felix Grzelka, and Patrick Baudisch. 2019. SpringFit: Joints and Mounts that Fabricate on Any Laser Cutter. In *Proceedings of the 32nd Annual ACM Symposium on User Interface Software and Technology*. 727–738.
- [30] Valkyrie Savage, Andrew Head, Björn Hartmann, Dan B Goldman, Gautham Mysore, and Wilmot Li. 2015. Lamello: Passive acoustic sensing for tangible input components. In *Proceedings of the 33rd Annual ACM Conference on Human Factors in Computing Systems*. 1277–1280.
- [31] Martin Schmitz, Jürgen Steimle, Jochen Huber, Niloofar Dezfali, and Max Mühlhäuser. 2017. Flexibles: deformation-aware 3D-printed tangibles for capacitive touchscreens. In *Proceedings of the 2017 CHI Conference on Human Factors in Computing Systems*. 1001–1014.
- [32] Christian Schumacher, Bernd Bickel, Jan Rys, Steve Marschner, Chiara Daraio, and Markus Gross. 2015. Microstructures to control elasticity in 3D printing. *ACM Transactions on Graphics (TOG)* 34, 4 (2015), 1–13.
- [33] Youngboe Aram Shim, Keunwoo Park, Sangyoon Lee, Jeongmin Son, Taeyun Woo, and Geehyuk Lee. 2020. FS-Pad: Video Game Interactions Using Force Feedback Gamepad. In *Proceedings of the 33rd Annual ACM Symposium on User Interface Software and Technology*. 938–950.
- [34] Ronit Slyper and Jessica Hodgins. 2012. Prototyping robot appearance, movement, and interactions using flexible 3d printing and air pressure sensors. In *2012 IEEE RO-MAN: The 21st IEEE International Symposium on Robot and Human Interactive Communication*. IEEE, 6–11.
- [35] Haruki Takahashi, Parinya Punpongson, and Jeejeun Kim. 2020. Programmable filament: Printed filaments for multi-material 3D printing. In *Proceedings of the 33rd Annual ACM Symposium on User Interface Software and Technology*. 1209–1221.
- [36] Anke van Oosterhout, Miguel Bruns, and Eve Hoggan. 2020. Facilitating Flexible Force Feedback Design with Feelix. In *Proceedings of the 2020 International Conference on Multimodal Interaction*. 184–193.
- [37] Anke van Oosterhout, Eve Hoggan, Majken Kirkegaard Rasmussen, and Miguel Bruns. 2019. DynaKnob: combining haptic force feedback and shape change. In *Proceedings of the 2019 on Designing Interactive Systems Conference*. 963–974.
- [38] Tatyana Vasilevitsky and Amit Zoran. 2016. Steel-sense: Integrating machine elements with sensors by additive manufacturing. In *Proceedings of the 2016 CHI Conference on Human Factors in Computing Systems*. 5731–5742.
- [39] Marynel Vázquez, Eric Brockmeyer, Ruta Desai, Chris Harrison, and Scott E Hudson. 2015. 3d printing pneumatic device controls with variable activation force capabilities. In *Proceedings of the 33rd Annual ACM Conference on Human Factors in Computing Systems*. 1295–1304.
- [40] Kentaro Yasu. 2019. Magnetact: magnetic-sheet-based haptic interfaces for touch devices. In *Proceedings of the 2019 CHI Conference on Human Factors in Computing Systems*. 1–8.
- [41] Clement Zheng, Jeejeun Kim, Daniel Leithinger, Mark D Gross, and Ellen Yi-Luen Do. 2019. Mechamagnets: Designing and fabricating haptic and functional physical inputs with embedded magnets. In *Proceedings of the Thirteenth International Conference on Tangible, Embedded, and Embodied Interaction*. 325–334.
- [42] Clement Zheng, HyunJoo Oh, Laura Devendorf, and Ellen Yi-Luen Do. 2019. Sensing kirigami. In *Proceedings of the 2019 on Designing Interactive Systems Conference*. 921–934.